NeuroImage 333 (2026) 121933

Contents lists available at ScienceDirect

NeuroImage

journal homepage: www.elsevier.com/locate/ynimg

Cortico-cortical paired associative stimulation highlights the functional role of the cortical pathway from the right inferior frontal gyrus to the primary motor cortex in motor inhibition

Naomi Bevacqua [a,b], Sonia Turrini [a], Antonio Cataneo [c], Sara Zago [d], Giorgio Arcara [c,d], Matteo Candidi [b], Giovanni Mirabella [e,f], Alessio Avenanti [a,g,*]

[a] Centro studi e ricerche in Neuroscienze Cognitive, Dipartimento di Psicologia "Renzo Canestrari", Alma Mater Studiorum—Università di Bologna, Campus di Cesena, Via Rasi e Spinelli 176, 47521 Cesena, Italy
[b] Dipartimento di Psicologia, Sapienza Università di Roma, 00185 Roma, Italy
[c] Department of General Psychology, University of Padova, 35131 Padua, Italy
[d] IRCCS San Camillo Hospital, Venice, Italy
[e] Department of Clinical and Experimental Sciences, University of Brescia, Brescia, Italy
[f] IRCCS Neuromed, 86077 Pozzilli, Italy
[g] Centro de Investigación en Neuropsicología y Neurociencias Cognitivas, Universidad Católica del Maule, 3460000 Talca, Chile

ARTICLE INFO

Keywords:
Motor inhibition
Cortico-cortical paired associative stimulation
Right inferior frontal gyrus
Primary motor cortex
Transcranial magnetic stimulation

ABSTRACT

Motor inhibition is the ability to suppress inappropriate motor responses. Dual-site transcranial magnetic stimulation studies suggest that the right inferior frontal gyrus (rIFG) can inhibit the primary motor cortex (M1), but it remains unclear whether inducing plasticity along this pathway affects motor inhibition. To address this issue, we used cortico-cortical paired associative stimulation (ccPAS) in healthy participants and assessed behavioral and electrophysiological markers of inhibition. In two sessions, we administered a ccPAS protocol to boost rIFG-M1 connections via Hebbian-like plasticity (ccPAS-rIFG-M1) and a reverse-order protocol (ccPAS-M1-rIFG) as a control. Consistent with well-documented inter-individual variability in response to brain stimulation, we divided participants into higher- and lower-sensitivity groups based on the progressive increase in motor excitability during ccPAS-rIFG-M1. Behavioral performance in the Go-NoGo task did not change as a function of ccPAS. However, independently of the ccPAS protocol, higher-sensitivity participants maintained an efficient proactive inhibitory strategy over time, whereas lower-sensitivity participants displayed increased response readiness at the expense of inhibitory control, suggesting stable individual differences rather than direct effects of stimulation. Furthermore, electrophysiological findings revealed that, following ccPAS-rIFG-M1, higher-sensitivity individuals showed a state-dependent increase of rIFG inhibitory influence over M1 only when viewing NoGo-cues. No comparable modulation was found for Go-cues, in lower-sensitivity individuals, or after ccPAS-M1-rIFG. These findings indicate that ccPAS-rIFG-M1 selectively modulates rIFG-M1 inhibitory interactions in a state- and sensitivity-specific manner, supporting a specific involvement of the targeted circuit in motor inhibition and linking individual plasticity capacity to stable differences in proactive inhibitory control.

1. Introduction

Motor inhibition refers to the ability to suppress, stop, or withhold inappropriate or prepotent motor responses in accordance with current goals and contextual demands (Ridderinkhof et al., 2004; Bari and Robbins, 2013; Aron et al., 2014). In motor tasks, two modes are commonly distinguished: reactive inhibition, the capacity to suppress a potential or prepotent response tendency in response to a stop signal, and proactive inhibition, a preparatory control process that biases response tendencies in advance according to goals and task demands (van den Wildenberg et al., 2022; Mirabella, 2023). Research on inhibitory control has identified a widespread network of cortical and subcortical areas (Borgomaneri et al., 2020; He et al., 2024), organized into a fronto-basal ganglia circuit responsible for response inhibition. An

* Corresponding author.
E-mail address: alessio.avenanti@unibo.it (A. Avenanti).

https://doi.org/10.1016/j.neuroimage.2026.121933
Received 11 September 2025; Received in revised form 1 April 2026; Accepted 15 April 2026
Available online 15 April 2026

extensive body of evidence has documented the involvement of the motor system during action stopping, as demonstrated by invasive single-unit recordings in non-human primates (Mirabella et al., 2011) and by human evidence from functional neuroimaging (i.e., Hamzei et al., 2002), electrocorticography (Mattia et al., 2012), and transcranial magnetic stimulation (TMS) (Arlati, Però et al., 2026). An influential model proposes that the primary motor cortex (M1) is modulated via a cortical-subcortical circuit, in which the right inferior frontal gyrus (rIFG) inhibits M1 via the right subthalamic nucleus (Aron, 2011). On the other hand, dual-site TMS (dsTMS) studies have provided evidence for a cortical-cortical pathway linking rIFG with the left M1 (Buch et al., 2010; Neubert et al., 2010; van Campen et al., 2013; Picazio et al., 2014). However, the functional role of such rIFG-to-M1 pathway in motor inhibition remains debated. The majority of the dsTMS experiments report that the rIFG exerts an inhibitory effect over the left M1 during action stopping or reprogramming (Buch et al., 2010; Neubert et al., 2010; Picazio et al., 2014). In contrast, van Campen and colleagues showed that the influence of the rIFG on M1 is strongly context-dependent: rIFG suppressed left M1 excitability during frequent NoGo trials, but not during infrequent NoGo trials, and facilitated left M1 excitability during all infrequent trials regardless of whether response inhibition was required (van Campen et al., 2013). This result aligns with accounts proposing that rIFG primarily supports attentional processes rather than acting as a purely inhibitory region (Hampshire et al., 2010; Sebastian et al., 2016).

More recently, Sel and colleagues (2021) employed cortico-cortical paired associative stimulation (ccPAS), a dsTMS protocol designed to induce Hebbian-like spike-timing-dependent plasticity (STDP) by repeatedly pairing stimulation of two interconnected areas (Rizzo et al., 2009; Hernandez-Pavon et al., 2023; Di Luzio et al., 2024). During a Go-NoGo task, strengthening rIFG-to-M1 connectivity increased frontocentral beta power during Go trials and theta power during NoGo trials, whereas weakening the rIFG-M1 pathway produced the opposite pattern (Sel et al., 2021). Effects induced by ccPAS were limited to physiological activity during the Go-NoGo task and did not impact performance. However, the functional meaning of the No-Go-related theta modulation remains ambiguous: theta oscillations have been linked not only to action inhibition (Prochnow et al., 2022) but also to attentional and cognitive control processes (Fiebelkorn and Kastner, 2019). As a consequence, these findings do not conclusively settle whether the rIFG primarily subserves motor inhibition or supports broader attentional functions. Crucially, these oscillatory effects did not directly establish the direction, sign, or causal influence of rIFG over M1 output.

To address these unresolved issues, here we combined dsTMS with a Go-NoGo task to investigate how directional effective connectivity from rIFG to the left M1 is modulated in a state-dependent manner during the observation of Go and NoGo cues. Using dsTMS, we probed in vivo the direction and sign of rIFG-to-M1 interactions while participants viewed stimuli signaling movement execution (Go) or withholding (NoGo). dsTMS provides a well-established method to assess effective cortico-cortical connectivity by comparing conditioned motor-evoked potentials (dsTMS-MEPs), elicited when a test TMS pulse over M1 is preceded by a conditioning TMS pulse over a connected cortical site, with non-conditioned responses elicited by single-pulse TMS over M1 alone (spTMS-MEPs) (Koch, 2020; Van Malderen et al., 2023). In the present study, the conditioning pulse was delivered over rIFG, such that effective connectivity was specifically assessed in the rIFG-to-M1 direction, allowing us to quantify the inhibitory and facilitatory causal influences exerted by rIFG over the left M1.

Crucially, beyond measuring state-dependent changes in rIFG-M1 connectivity, we also manipulated this circuit using ccPAS. By inducing Hebbian-like plasticity along the rIFG-M1 pathway, we tested whether strengthening rIFG-to-M1 connectivity selectively alters (i) rIFG influence on the left M1, indexed by dsTMS-MEPs, and (ii) behavioral motor inhibition during the Go-NoGo task. This allowed us to assess the functional relevance of rIFG-M1 connectivity at the neural level, while also exploring whether such modulation translates into measurable behavioral changes. This combined approach provides a direct test of the functional contribution of the rIFG-M1 pathway to motor inhibition, thereby helping to disentangle inhibitory from attentional accounts of IFG function.

Based on the hypothesis that rIFG plays a primary role in motor inhibition, we predicted that strengthening its connectivity with the left M1 (through $ccPAS_{rIFG\text{-}M1}$) would modulate inhibitory processing, primarily reflected at the level of effective connectivity, and potentially at the behavioral level. Specifically, we expected a state-dependent modulation of effective connectivity as reflected by dsTMS-MEPs: during NoGo trials, we anticipated a strengthened inhibitory influence of rIFG over the left M1. In contrast, during Go trials, we expected either no modulation or a relative release from inhibition. A selective increase of inhibition during NoGo trials would support the hypothesis that rIFG directly contributes to motor inhibition through its influence on M1, whereas a bidirectional modulation of rIFG-M1 interactions (inhibition during NoGo and facilitation during Go) would be more consistent with accounts proposing that rIFG primarily supports attentional or contextual control processes. In addition, based on previous evidence showing either null or small effects in the opposite direction when ccPAS is applied in the reverse order (Di Luzio et al., 2024), we did not expect reliable changes after the control stimulation ($ccPAS_{M1\text{-}rIFG}$).

Finally, in line with a growing body of evidence documenting substantial interindividual variability in responses to brain stimulation (Hamada et al., 2013; López-Alonso et al., 2014; Vallence et al., 2015; Valchev et al., 2017; Paracampo et al., 2018), including ccPAS targeting of IFG/ventral premotor cortex and M1 (Turrini et al., 2023a), and the possibility to assess ccPAS physiological effects in real time (Turrini et al., 2022, 2025; Bevacqua et al., 2024), we explicitly took individual differences in online physiological responsiveness to $ccPAS_{rIFG\text{-}M1}$ into account. Rather than treating this variability as mere noise, we leveraged differences in $ccPAS_{rIFG\text{-}M1}$ responsiveness to stratify participants into higher- and lower-sensitivity groups. Importantly, interindividual variability served two complementary purposes. First, it allowed us to test whether any causal effects of $ccPAS_{rIFG\text{-}M1}$ on state-dependent rIFG-M1 effective connectivity during Go and NoGo cue processing, as well as on behavioral performance in the Go-NoGo task, were more evident in higher-sensitivity individuals. Second, it allowed us to characterize trait-like differences between individuals by examining whether higher- and lower-sensitivity participants also differed in their overall inhibitory performance, independently of stimulation effects. In this way, ccPAS-induced physiological modulation was used as a putative marker of the capacity of the rIFG-M1 pathway to express Hebbian-like plasticity. If greater plasticity reflects, at least in part, greater functional engagement of the pathway (Freitas et al., 2013; Stampanoni Bassi et al., 2019), and if that pathway supports motor inhibition, then interindividual differences in ccPAS sensitivity may be associated with differences in neural reactivity to Go and NoGo cues and, potentially, in task performance (Turrini et al., 2023a).

2. Materials and Methods

2.1. Participants

30 healthy volunteers were recruited for this study at the Center for studies and research in Cognitive Neuroscience, University of Bologna, Cesena Campus; two dropped out before completing the two experimental sessions, resulting in a sample of 28 Italian undergraduate students (mean age: 23.79 ± SD: 2.81; 17 females). We chose this sample size coherently with the other studies that used ccPAS (Di Luzio et al., 2024). All participants were right-handed, based on the Edinburgh Handedness Inventory (Oldfield, 1971) and had a normal or corrected-to-normal vision. Before beginning the experiment, all volunteers gave informed consent and were screened to avoid adverse

reactions to TMS (Rossi et al., 2022). All the experimental procedures were performed following the 1964 Declaration of Helsinki and later amendments (WMA, 2013) and approved by the local Bioethics Committee of the University of Bologna (Protocol number 284747). No adverse reactions or discomfort related to the TMS were reported by participants or noticed by the experimenters.

2.2. General experimental design

The experiment had a within-subjects design consisting of two sessions with the same structure (Fig. 1A), separated by at least one week. In one session, participants underwent rIFG-to-M1 ccPAS (ccPAS$_{rIFG\text{-}M1}$), designed to transiently enhance rIFG-to-M1 effective connectivity by repeatedly stimulating the input cortical site (rIFG) just before the output cortical site (left M1), consistent with spike-timing-dependent (Hebbian-like) plasticity mechanisms (Bi and Poo, 2001). In the other session, participants underwent M1-to-rIFG ccPAS (ccPAS$_{M1\text{-}rIFG}$), in which the stimulation order was reversed while all other stimulation parameters remained constant, thereby serving as a control condition for the temporal-order specificity of ccPAS effects. The order of the two sessions was counterbalanced across participants. Each session started with an electrophysiological preparation consisting of the electromyographic (EMG) electrodes montage, motor hot spot, resting motor threshold (rMT) detection, and the identification of the TMS intensity required to reliably elicit MEPs of approximately 1 mV amplitude in the target muscle ($SI_{1\ mV}$; see TMS and EMG recording paragraph). At baseline, before any behavioral task session or ccPAS intervention, we assessed the neurophysiological response of the motor system to the visual cues later used as Go and NoGo stimuli in the behavioral task. This evaluation included measuring corticospinal excitability through single-pulse TMS (spTMS) MEPs and assessing cortico-cortical effective connectivity via dsTMS over the IFG-M1 pathway (see TMS Block Procedure section). Following these assessments, participants completed the baseline block of the Go-NoGo task (see Go-NoGo Task section). Subsequently, we administered a 15-minute ccPAS protocol over right IFG and left M1 (either ccPAS$_{rIFG\text{-}M1}$ or ccPAS$_{M1\text{-}rIFG}$) to repeatedly activate the neural pathway connecting these regions and modulate its functional strength (Di Luzio et al., 2024). Participants were asked to perform the Go-NoGo task immediately after (T-0) and 30 min after (T-30) the end of ccPAS, consistent with the timing of the ccPAS stimulation effect (Di Luzio et al., 2024). Finally, the experiment ended with a final TMS block where the corticospinal excitability (spTMS-MEPs) and cortico-cortical connectivity (dsTMS-MEPs) in response to the Go and NoGo visual cues were assessed again. These measurements were taken approximately 40 min after the end of the ccPAS (T-40), aligning with previous studies which reported a progressive build-up of ccPAS-driven plastic effects in the motor system (Arai et al., 2011; Lu et al., 2012; Chao et al., 2015; Fiori et al., 2018; Turrini et al., 2023b).

2.3. TMS block procedure

Participants were seated comfortably on a chair and instructed to maintain their right hand relaxed while looking at a computer screen positioned approximately 80 cm away, where blue or red squares (200×200 pixels; corresponding to ~3.34°×3.34° of visual angle) appeared in random order. The TMS block consisted of 16 spTMS and 16 dsTMS trials for each visual cue type, presented in a fully randomized order. In dsTMS trials, stimulation of M1 was preceded by a conditioning TMS pulse over the IFG, 8 ms before the test pulse on M1 (Buch et al., 2010). To maintain attentional engagement, 4 catch trials were interspersed throughout each block. During these trials, a number was briefly displayed instead of a colored square, and participants were instructed to read it aloud (total number of trials: 68). Each trial started with a

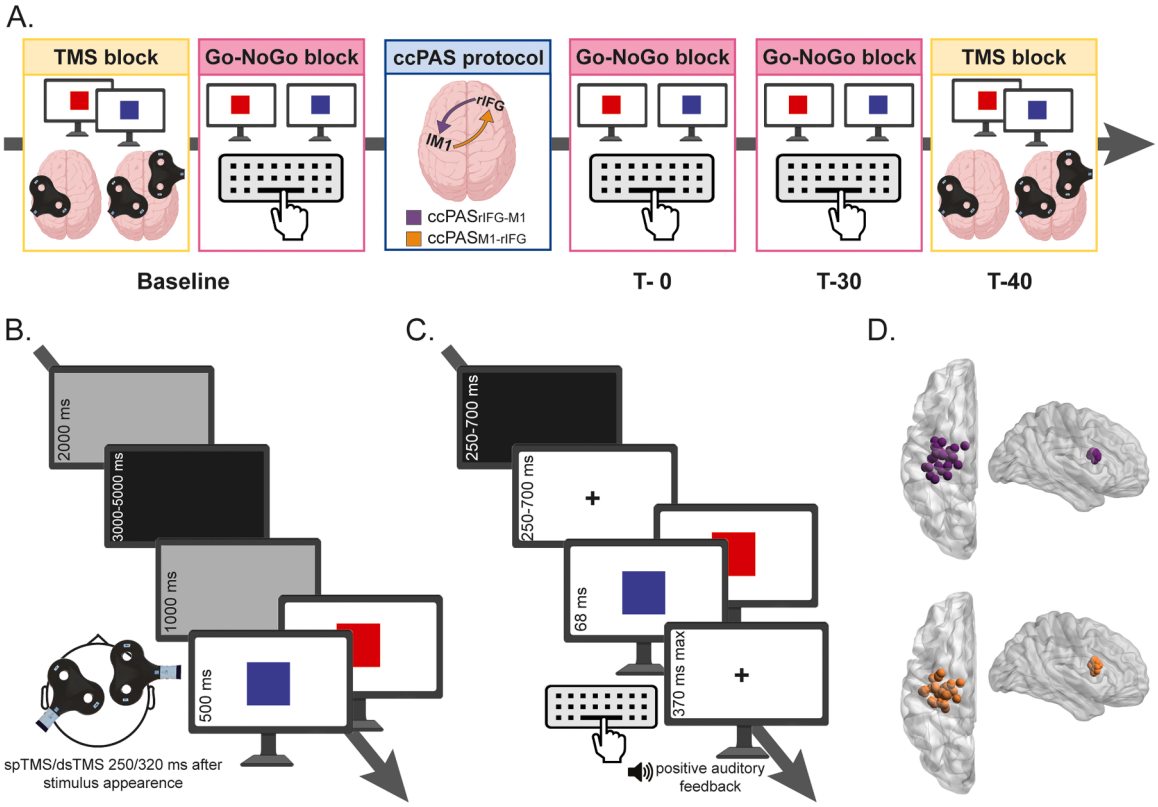

Fig. 1. A. General Experimental Design. B. Outline of TMS block trials. C. Outline of one Go-NoGo task trial. D. Stimulation spot for each participant, in purple for the ccPAS$_{rIFG\text{-}M1}$ session and in orange for the ccPAS$_{M1\text{-}rIFG}$ session; all participants took part in two sessions and received both stimulations in counterbalanced order (at least 1-week apart). Abbreviations: spTMS: single-pulse TMS; dsTMS: dual-site TMS.

black screen (random duration ranging between 3000–5000 ms) followed by a grey screen (1000 ms duration), the colored visual cue (500 ms) and a grey screen again (2000 ms). The TMS pulses were administered while the colored square was displayed, either 250 or 320 ms after their appearance. Therefore, TMS pulses were separated by a random time ranging from 6500 to 8500 ms (Fig. 1B).

2.4. Go-NoGo Task

The Go-NoGo task consisted of 400 trials, with a short break halfway through. Trials were presented on a computer screen ~80 cm away from the participant. Each trial began with a black screen (250–700 ms), followed by a white screen with a black fixation cross (250–700 ms). Subsequently, a red or a blue square (200×200 pixels) was displayed for 68 ms, then the screen returned to white. Participants were instructed to respond by pressing the space bar with their right index finger within 370 ms when the Go cue was presented, and refrain from responding when the NoGo cue was presented. To induce a prepotent tendency to respond, the rate of the Go trial was set at 80 % of the total trials (Wessel, 2018; Young et al., 2018). The visual cues assigned to Go and NoGo commands were counterbalanced across participants. If the trial was correctly completed (i.e., response within 370 ms for Go trials and no response in NoGo trials), participants received positive audio feedback. In the event of a failed trial (i.e., omission error or commission error), participants did not receive the feedback (Fig. 1C). Reaction times (RTs) in correct trials and omission error rate (i.e., failures to press the button in Go trials) were recorded as a measure of response readiness, and commission error rate was recorded as a measure of reactive motor inhibition (Ren et al., 2023).

2.5. ccPAS Procedure

The ccPAS consisted of 15 min of dsTMS delivered over the selected IFG and M1 sites at 0.1 Hz frequency (i.e., 90 pairs of pulses), with an interstimulus interval of 8 ms (Sel et al., 2021; Lazari et al., 2022), to activate short latency connections between the two areas (Buch et al., 2010; Turrini et al., 2023c; Chiappini et al., 2025). During the protocol, we stimulated the IFG region with a subthreshold intensity (90 % of the rMT), while applying a suprathreshold intensity to the M1 hotspot at an intensity sufficient to produce 1 mV MEPs. This enabled the recording of 90 MEPs, one for each paired stimulation (Turrini et al., 2022, 2023b; Bevacqua et al., 2024).

2.6. TMS and EMG recording

TMS was performed using two 50-mm figure-of-eight iron branding coils, with the handles perpendicular to the plane of the wings, connected to two separate Magstim 200^2 monophasic stimulators (The Magstim Company, UK). The experiment started with the electrode montage setup, detection of optimal scalp position, and determination of TMS intensity. Ag/AgCl surface electrodes were placed over the right first dorsal interosseus (FDI) muscle using a belly-tendon montage, with ground electrodes placed on the right wrist. EMG signals were recorded using a Biopac MP-35 (Biopac, U.S.A.) electromyograph, band-pass filtered between 30 and 500 Hz, sampled at 10 kHz, digitized, and stored for offline analysis. The left M1 coil was held tangentially to the scalp at an angle of 45° from the midline to induce a posterior-to-anterior current in the brain (Kammer et al., 2001; Di Lazzaro et al., 2004). The optimal M1 scalp position, defined as the site eliciting the largest MEPs in the right FDI, was identified and marked on a swim cap to ensure consistent coil placement throughout the experiment. Resting motor threshold (rMT) was defined as the minimum intensity of the stimulator output eliciting MEPs with an amplitude of at least 50 μV in 5 out of 10 consecutive trials (Rossini et al., 2015). Stimulation intensity was then adjusted to evoke MEPs with an average peak-to-peak amplitude of ~1 mV (SI_{1mV}) (for mean rMT and SI_{1mV} values across sessions see Table 1).

For both the TMS Blocks and ccPAS protocols, the M1 site was located functionally as described above and stimulated at SI_{1mV} (Buch et al., 2011; Johnen et al., 2015; Fiori et al., 2018; Turrini et al., 2022). The rIFG site, corresponding to the caudal portion of the pars opercularis, was identified through a neuronavigation system (see next paragraph). The rIFG coil was placed tangentially to the scalp, inducing a posterior-to-anterior and lateral-to-medial current flow, in the direction of M1. The intensity of rIFG stimulation was adjusted to 90 % of each participant's rMT (Turrini et al., 2022, 2024, 2025; Bevacqua et al., 2024; Chiappini et al., 2024). The effectiveness of subthreshold conditioning is supported by ccPAS studies (Di Luzio et al., 2024) and dsTMS studies testing ventral premotor cortex (PMv)/IFG-to-M1 interactions (Davare et al., 2008, 2009, 2010; Bäumer et al., 2009; Fiori et al., 2016, 2017; Chiappini et al., 2025; Bevacqua et al., 2026). Pulses were remotely triggered by a MATLAB script (MathWorks, Natick, USA). To minimize potential discomfort, participants received 4–5 test pulses of increasing intensity over the rIFG before the experiment.

2.7. Neuronavigation

The rIFG site was identified using the SofTaxic Navigator System (Electro Medical System, Bologna, IT). Skull landmarks (2 preauricular points, nasion and inion) and ~80 points were digitized using a Polaris Vicra digitizer (Northern Digital). We obtained an estimated MRI via a 3D warping procedure that fit a high-resolution MRI template to each participant's scalp and craniometric points. To target the rIFG, we used the following Talairach coordinates: $x = 53$; $y = 10$; $z = 19$, consistent with previous studies (Buch et al., 2011; Picazio et al., 2014; Sel et al., 2021; Trajkovic et al., 2023). For each participant, the Talairach coordinates corresponding to the projections of the rIFG and M1 scalp sites onto the brain surface were estimated by the SofTaxic Navigator from the MRI-constructed stereotaxic template. The resulting projected coordinates are consistent with the area 44/pars opercularis for the rIFG site and with M1 for the motor target (Tomaiuolo et al., 1999; Mayka et al., 2006) (see Table 2 and Fig. 1D).

3. Statistical analyses

3.1. Preliminary analyses

Neurophysiological data were processed offline. MEP peak-to-peak amplitudes were extracted in a time window of 60 ms, starting 15 ms after the TS through custom MATLAB code (Turrini, 2023). Since background EMG affects motor excitability (Devanne et al., 1997), MEPs preceded by background EMG activity deviating from the individual mean of the block by >2 SD were discarded from the analysis. Moreover, MEPs deviating from the mean amplitude of their test block by >3 SD were discarded (6 % of MEPs excluded in total). spTMS MEPs and the dsTMS MEPs were expressed in mV, while %dsTMS MEPs were calculated as the ratio of the mean of dsTMS MEPs over the mean of spTMS MEPs amplitude for each stimulus, as typically done to index facilitatory/inhibitory effects due to inter-areal effective connectivity tested through dsTMS over spTMS (Davare et al., 2008, 2009; Buch et al., 2010, 2011; Chiappini et al., 2020, 2024). To ensure that there were no

Table 1
Mean TMS intensity parameters (± SD) across the two sessions. rMT = resting motor threshold; SI_{1mV} = stimulation intensity required to elicit MEPs of ~1 mV; values are expressed as % of maximum stimulator output. No significant between-session differences were found for either rMT or SI_{1mV}.

	rMT	SI_{1mV}
$ccPAS_{rIFG\text{-}M1}$	46.6 ± 7.6	58.6 ± 10.1
$ccPAS_{M1\text{-}rIFG}$	42.8 ± 13.4	53.5 ± 17.2
Statistical Analysis	$F_{1,27} = .02$; $p = .88$	$F_{1,27} = .67$; $p = .42$

Table 2
Mean (±SD) Talairach coordinates (mm) of targeted sites in the two experimental sessions.

	M1			IFG		
	x	y	z	x	y	z
ccPAS$_{rIFG-M1}$	−32 ± 8	−14 ± 12	56 ± 6	54 ± 3	10 ± 2	20 ± 9
ccPAS$_{M1-rIFG}$	−32 ± 8	−16 ± 10	57 ± 6	54 ± 2	10 ± 2	18 ± 3
Statistical Analysis	all $F \leq 2.13$, all $p \geq .16$					

differences in motor excitability across the two sessions, *t*-tests were performed on rMT and SI_{1mV} values (Table 1).

As accuracy measures, we collected and analyzed the commission error rate (i.e., the percentage of NoGo trials in which the subject pressed the space bar although they should not) and the omission error rate (i.e., the percentage of Go trials in which the subject did not press the space bar within 370 ms). For response speed, we analyzed the RTs in correct trials after discarding all trials that deviated >3 SD from the mean of the block, which were considered as outliers.

3.2. Analysis of online effects of ccPAS

To test the online effect of the ccPAS on motor excitability, we analyzed the 90 MEPs collected during the stimulation phase. MEPs were divided into 9 consecutive epochs of 10 MEPs each. A two-way repeated measures ANOVA was conducted with the within-subjects factors ccPAS protocol (2 levels: ccPAS$_{rIFG-M1}$; ccPAS$_{M1-rIFG}$) and Epoch (9 levels). As shown in the Results section, this analysis revealed a significant interaction between the two factors, showing a progressive increase in the motor excitability across epochs during ccPAS$_{rIFG-M1}$, reflecting the growing influence of rIFG on M1 and interpreted as a proxy of the protocol's efficacy in inducing cortico-cortical plasticity (Turrini et al., 2023a,b; Bevacqua et al., 2024). Given the observed interindividual variability in the magnitude of this effect, we further categorized participants according to the slope of their MEP amplitude change across the 9 epochs during ccPAS$_{rIFG-M1}$, distinguishing between a "higher-sensitivity" group (slopes above the median; median = .04) and a "lower-sensitivity" group (slopes below the median). The higher-sensitivity and lower-sensitivity groups did not differ in terms of age, rMT, and M1 coordinates (all $F \leq .58$; all $p \geq .45$; Table 3). Finally, to explore the role of individual physiological responsiveness to ccPAS in modulating ccPAS effects, we ran a further ANOVA including the between-subjects factor ccPAS-sensitivity (2 levels: Higher, Lower). This analysis revealed the higher-order interaction, which was explored by running two separate Epoch x ccPAS-sensitivity ANOVAs, one for each ccPAS protocol.

3.3. Behavioral analyses

Behavioral data (commission error rate, omission error rate, RTs) were normally distributed, thus each measure was submitted to a separate two-way ANOVA, with the within-subjects factors ccPAS protocol (2 levels: ccPAS$_{rIFG-M1}$, ccPAS$_{M1-rIFG}$) and Time (3 levels: Baseline, T-0, T-30), which showed changes in performance at T-30 across groups. To test the influence of individual ccPAS-responsiveness, we also repeated the analysis including the between-subject factor ccPAS-sensitivity (2 levels: Higher, Lower; see paragraph #3.2), focusing on MEPs changes between Baseline and T-30.

Table 3
Mean ± SD of age (years), rMT (% of maximal stimulator output), and M1 Talairach coordinates (mm) in the two groups of participants.

	Age	rMT	M1 coordinates		
			x	y	z
Higher-sensitivity group	24 ± 2	47 ± 9	−31 ± 8	−13 ± 12	56 ± 5
Lower-sensitivity group	24 ± 4	45 ± 5	−33 ± 9	−16 ± 10	56 ± 6

3.4. Corticospinal excitability (spTMS MEPs) analysis

Inspection of the data revealed that spTMS MEP amplitudes were not normally distributed. Consequently, data were analyzed through non-parametric tests. Friedman tests were used to compare MEPs recorded during the vision of Go and NoGo cues at Baseline and T-40 timepoints, separately for higher-sensitivity and lower-sensitivity subgroups. Kruskal-Wallis tests were used to compare the two subgroups across the different conditions.

3.5. Effective rIFG-M1 connectivity (%dsTMS MEPs) analysis

%dsTMS MEPs data were normally distributed and were analyzed by means of a four-way repeated measures ANOVA with the within-subjects factors ccPAS protocol (2 levels: ccPAS$_{rIFG-M1}$, ccPAS$_{M1-rIFG}$), Stimulus (2 levels: Go, NoGo), and Time (2 levels: Baseline, T-40), and the between-subjects factor ccPAS-sensitivity (2 levels: Higher, Lower). The ANOVA revealed the higher-order interaction, explored through two separate three-way ANOVAs, one for each ccPAS protocol, with within-subjects factors Stimulus (2 levels: Go, NoGo) and Time (2 levels: Baseline, T-40), and between-subjects factor ccPAS-sensitivity (2 levels: Higher, Lower). Finally, to better characterize the inhibitory conditioning effect of the IFG on the M1 when viewing NoGo visual cues following ccPAS$_{rIFG-M1}$ at T-40, we conducted a paired-samples *t*-test comparing spTMS MEPs and dsTMS MEPs (expressed in millivolts rather than as a percentage) in higher-sensitivity participants.

3.6. Follow-up analyses and measures of effect size

All significant interactions in the ANOVAs were explored through trend analyses and planned comparisons. The trend analysis was conducted on MEPs and behavioral performance metrics to evaluate changes over time. For physiological modulation, we examined differences between Baseline and T-40 for both visual cues, while behavioral performance at Baseline was compared with that at T-30.

For all ANOVAs, the partial eta squared (η_p^2) was computed as an effect size metric for all significant effects; η_p^2 effect sizes of ~.01, ~.06, and ~.14 are conventionally considered small, medium, and large. For significant planned comparisons, we reported the F value, p value, and the η_p^2. For non-parametric analyses, Kendall's W was used as the effect size measure for Friedman tests. W values of approximately .10, .30, and .50 were interpreted as small, moderate, and large, respectively. In addition, eta squared based on the Kruskal-Wallis H statistic (η_H^2) was used for between-group comparisons, following recommendations for reporting effect sizes with non-parametric tests (Tomczak and Tomczak, 2014). All the analyses were performed with STATISTICA version 12.

4. Results

4.1. Corticomotor excitability during ccPAS

The ANOVA on spMEPs during ccPAS revealed a significant ccPAS protocol x Epoch interaction with medium/large effect size ($F_{8,216} = 2.65$; $p = .009$; $\eta_p^2 = .09$; Fig.2A). The trend analysis showed that MEPs significantly increased during the ccPAS$_{rIFG-M1}$ ($F_{1,27} = 10.32$; $p = .003$; $\eta_p^2 = .28$). A linear fit of the epoch means showed a positive slope (slope = .086; $R^2 = .89$). No linear trend emerged during the ccPAS$_{M1-rIFG}$ ($F_{1,27} = .21$; $p = .65$; $\eta_p^2 = .01$), and the fitted slope was close to zero (slope = .009; $R^2 = .06$). Yet, since the response to ccPAS$_{rIFG-M1}$ was variable across individuals, we divided our sample into higher-sensitivity and

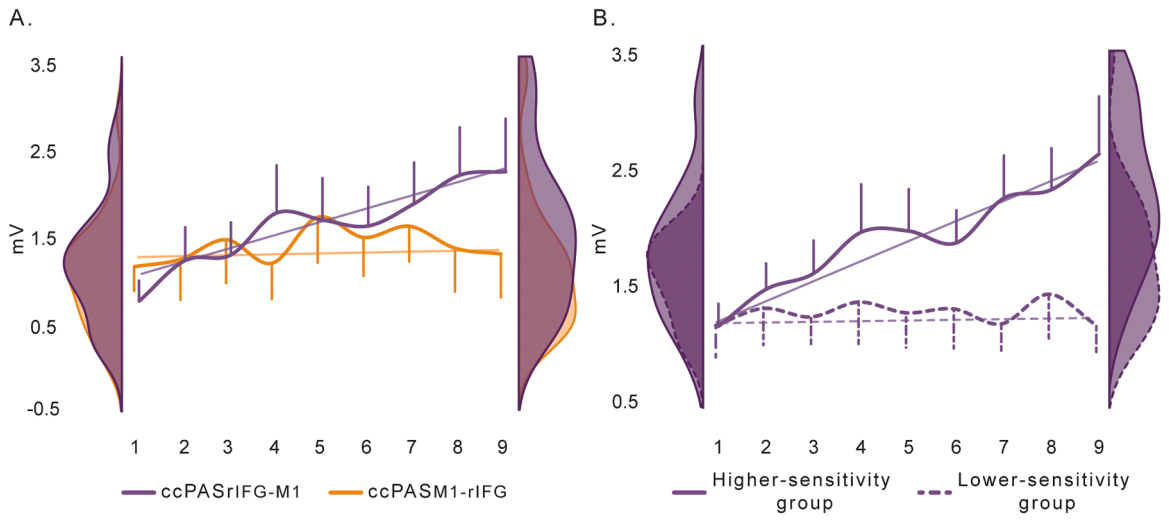

Fig. 2. A. MEPs during $ccPAS_{rIFG\text{-}M1}$ (purple line) and $ccPAS_{M1\text{-}rIFG}$ (orange line). B. On the right MEPs during $ccPAS_{rIFG\text{-}M1}$ in higher-sensitivity (continuous line) and lower-sensitivity participants (dashed line). The half violins represent the data distribution. Error bars represent 1 SEM. The straight lines represent the linear fitting of the MEPs modulation. (For interpretation of the references to color in this figure legend, the reader is referred to the web version of this article.).

lower-sensitivity subgroups (see Statistical Analyses) and conducted an ANOVA incorporating the factor Sensitivity, which revealed a significant three-way interaction ccPAS protocol x Epoch x ccPAS-sensitivity ($F_{8,208} = 2.86$; $p = .005$; $\eta_p^2 = .09$). The ANOVA on $ccPAS_{rIFG\text{-}M1}$ MEPs revealed a significant main effect of Epoch ($F_{8,208} = 4.94$; $p < .001$; $\eta_p^2 = .16$), qualified by the Epoch x ccPAS-sensitivity interaction ($F_{8,208} = 4.35$; $p < .001$; $\eta_p^2 = .14$; Fig.2B). A trend analysis showed that in higher-sensitivity participants MEPs increased during the $ccPAS_{rIFG\text{-}M1}$ ($F_{1,26} = 28.20$; $p < .001$; $\eta_p^2 = .52$), fitting a linear distribution (slope = .17; $R^2 = .93$); in contrast, lower-sensitivity participants did not show changes of the MEPs during the ccPAS protocol ($F_{1,26} = .03$; $p = .87$, $\eta_p^2 = .001$), and the fitted slope was close to zero (slope = .005; $R^2 = .02$). Moreover, although the two groups did not differ in the first epoch ($F_{1,26} < .001$; $p = .98$; $\eta_p^2 < .001$), a significant difference was observed in the final epoch ($F_{1,26} = 7.03$; $p = .01$; $\eta_p^2 = .21$). No significant results emerged from the ANOVA on MEPs recorded during $ccPAS_{M1\text{-}rIFG}$ (all $F \leq 3.97$; all $p \geq .06$; all $\eta_p^2 \leq .13$).

4.2. Behavioral effects of ccPAS

ANOVAs on correct RTs, commission, and omission error rates revealed a large effect of Time. Over time, participants made more commission errors (Baseline: 34% ± 14%; T-30: 40% ± 18%; $F_{2,54} = 10.19$; $p < .001$; $\eta_p^2 = .16$; Fig. 3A), fewer omission errors (Baseline: 5% ± 2%; T-30: 3% ± 2%; $F_{2,54} = 13.06$; $p < .001$; $\eta_p^2 = .19$; Fig. 3B), and became faster (Baseline: 256 ± 17 ms; T-30: 246 ± 20 ms; $F_{2,54} = 14.53$; $p < .001$; $\eta_p^2 = .21$; Fig. 3C). Critically, these effects were similar across the two ccPAS conditions, as the ccPAS protocol did not interact with the other factors in the ANOVA (all $F \leq .92$; all $p \geq .41$; all $\eta_p^2 \leq .03$).

In the analyses including the factor ccPAS-sensitivity, the ANOVAs on RTs and omission error rates again confirmed a strong effect of Time (all $F \geq 17.06$; all $p < .001$; all $\eta_p^2 \geq .40$), but did not reveal an influence of ccPAS-sensitivity (all $F \leq 1.17$; all $p \geq .17$; all $\eta_p^2 \leq .07$; Fig. 3E–F). In contrast, a significant Time x ccPAS-sensitivity interaction with large effect size emerged for commission error rates ($F_{1,26} = 4.57$; $p = .04$; $\eta_p^2 = .15$; Fig. 3D), indicating that the change over time differed between the two groups. While commission errors markedly increased in lower-sensitivity participants from Baseline (38 % ± 15 %) to T-30 (48 % ± 19 %; $F_{1,26} = 19.84$; $p < .001$; $\eta_p^2 = .43$), they did not change in the higher-sensitivity group (Baseline: 30 % ± 15 %; T-30: 33 % ± 13 %; $F_{1,26} = 2.05$; $p = .16$; $\eta_p^2 = .07$); moreover, while the two groups did not differ at baseline ($F_{1,26} = 2.45$; $p = .13$; $\eta_p^2 = .09$), at T-30 lower-sensitivity participants made more commission errors compared to higher-sensitivity participants ($F_{1,26} = 5.78$; $p = .02$; $\eta_p^2 = .18$). This pattern suggests that response readiness increased over time in both groups, as reflected by faster responses and fewer omission errors. However, only lower-sensitivity participants showed a speed-accuracy trade-off, with increased response readiness occurring at the expense of inhibitory control. In contrast, higher-sensitivity participants showed a genuine performance improvement, with enhanced response readiness accompanied by preserved inhibitory control, suggesting better proactive control over response tendencies. These effects were observed following both ccPAS protocols ($ccPAS_{rIFG\text{-}M1}$, $ccPAS_{M1\text{-}rIFG}$) as suggested by the non-significant Responsiveness x Time x ccPAS protocol interaction ($F_{1,26} = .02$; $p = .88$; $\eta_p^2 < .001$).

4.3. Effects of ccPAS on corticospinal response to Go and NoGo visual cues

At Baseline, spTMS-MEPs recorded during the observation of Go and NoGo cues did not differ between higher- and lower-sensitivity participants, either in the $ccPAS_{rIFG\text{-}M1}$ session (all $H \leq 2.03$; all $p \geq .15$; all $\eta_H^2 \leq .04$) or in the $ccPAS_{M1\text{-}rIFG}$ session (all $H \leq 2.30$; all $p \geq .13$; all $\eta_H^2 \leq .05$). Critically, spTMS MEP amplitudes for both visual cues did not vary across timepoints and ccPAS sessions in both the higher- ($\chi^2 = 9.93$; $p = .19$; $W = .10$) and lower-sensitivity ($\chi^2 = 2.33$; $p = .94$; $W = .02$) groups (Table 4).

4.4. Effects of ccPAS on effective IFG-M1 connectivity during Go and NoGo visual cues

The ANOVA on %dsTMS-MEPs revealed a significant 4-way ccPAS protocol x Stimulus x Time x ccPAS-sensitivity interaction ($F_{1,26} = 4.55$; $p = .04$; $\eta_p^2 = .15$). The Stimulus x Time x ccPAS-sensitivity ANOVA on the $ccPAS_{rIFG\text{-}M1}$ showed a significant 3-way interaction with large effect size ($F_{1,26} = 4.54$; $p = .04$; $\eta_p^2 = .15$; Fig.4A). At Baseline, %dsTMS-MEPs did not differ between groups, nor between Go and NoGo visual cues within each group (all $F \leq 1.67$; all $p \geq .39$). Importantly, in higher-sensitivity participants, %dsTMS-MEPs were modulated in a state-dependent way: %dsTMS-MEPs displayed an amplitude decrease when viewing NoGo visual cues at T40 (86 % ± 26 %) relative to Baseline (111 % ± 49 %; $F_{1,26} = 4.16$; $p = .05$; $\eta_p^2 = .14$); in contrast, %dsTMS-MEPs during Go visual cues did not show differences between Baseline (101 % ± 30 %) and T40 (116 % ± 40 %; $F_{1,26} = 1.67$; $p = .20$; $\eta_p^2 = .06$), however, at T40, %dsTMS-MEPs were lower when viewing NoGo relative to Go visual cues ($F_{1,26} = 5.66$; $p = .02$; $\eta_p^2 = .18$). In addition, a

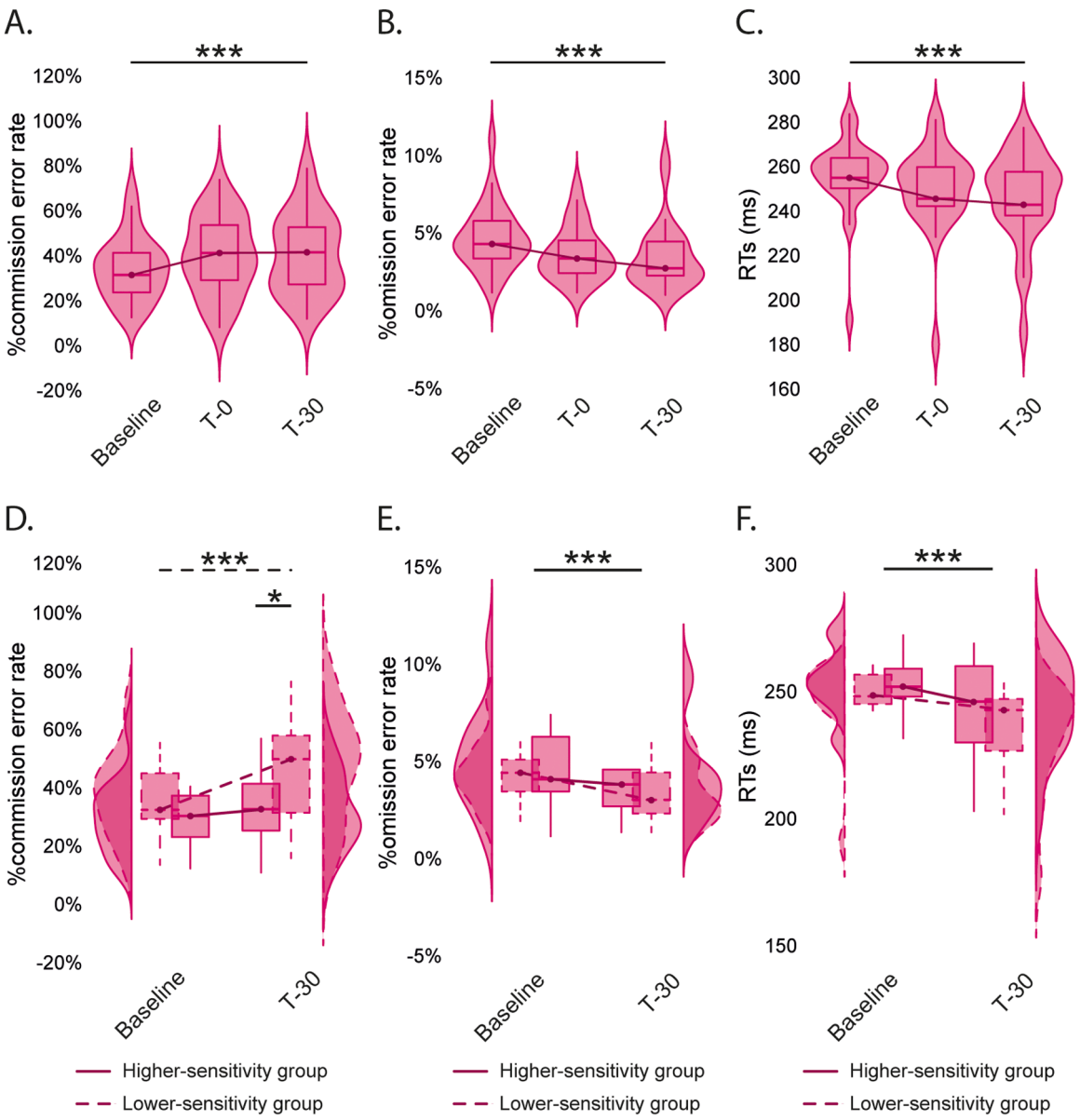

Fig. 3. Commission error rate (**A**), omission error rate (**B**), and RTs (**C**) over time across all participants. Commission error rate (**D**), Omission error rate (**E**), and RTs (**F**) over time in higher-sensitivity participants (continuous line) and lower-sensitivity participants (dashed line). Box plots represent the mean, first and third quartiles, and the 95 % confidence interval of individual data points. Half-violins represent data distribution. Asterisks indicate significant post-hoc comparison: * = $p \leq .05$, *** = $p \leq .001$.

Table 4
Mean MEP amplitudes (±SD) induced by spTMS at baseline in the two groups of participants.

		Higher-sensitivity	Lower-sensitivity
ccPAS$_{rIFG\text{-}M1}$	Go stimulus Baseline	1.43 ± .62 mV	1.20 ± .75 mV
	Go stimulus T40	1.45 ± 1.03 mV	1.35 ± .98 mV
	NoGo stimulus Baseline	1.28 ± .53 mV	1.22 ± .63 mV
	NoGo stimulus T40	1.76 ± 1.12 mV	1.31 ± .99 mV
ccPAS$_{M1\text{-}rIFG}$	Go stimulus Baseline	1.36 ± 1.12 mV	.90 ± .24 mV
	Go stimulus T40	1.49 ± 1.02 mV	1.18 ± .57 mV
	NoGo stimulus Baseline	1.70 ± 1.35 mV	.95 ± .33 mV
	NoGo stimulus T40	1.63 ± 1.14 mV	1.13 ± .64 mV

series of paired-sample *t*-tests comparing spTMS-MEPs and dsTMS-MEPs associated with the NoGo visual cue further confirmed that dsTMS-MEP amplitudes were significantly lower than spTMS-MEP amplitudes at T-40 (spTMS MEPs: 1.76 ± 1.12 mV, dsTMS-MEPs: 1.49 ± 1.06 mV; $t_{13} = 2.34$; $p = .03$; $\eta_p^2 = .30$; Fig. 5), whereas no significant difference emerged between spTMS-MEPs and dsTMS-MEP amplitudes at Baseline (spTMS MEPs: 1.28 ± .53 mV, dsTMS-MEPs: 1.34 ± .62 mV; $t_{13} = -0.62$; $p = .54$; $\eta_p^2 = .03$). Thus, the selective reduction of %dsTMS-MEPs during NoGo trials indicates a state-dependent increase in the inhibitory influence of rIFG over the left M1 corticospinal excitability in higher-sensitivity participants. In contrast, no modulation of %dsTMS-MEPs was observed in lower-sensitivity participants (all $F \leq .35$; all $p \geq .57$; all $\eta_p^2 \leq .01$; Fig.4B), or following ccPAS$_{M1\text{-}rIFG}$ (all $F \leq 2.57$: all $p \geq .12$; all $\eta_p^2 \leq .09$; Fig.4C-D).

5. Discussion

Correlational evidence from neuroimaging studies shows increased activity of the frontal cortices, such as rIFG and supplementary motor areas, during the suppression or reprogramming of motor acts (Stinear et al., 2009; Swann et al., 2012). Moreover, single-unit recordings in

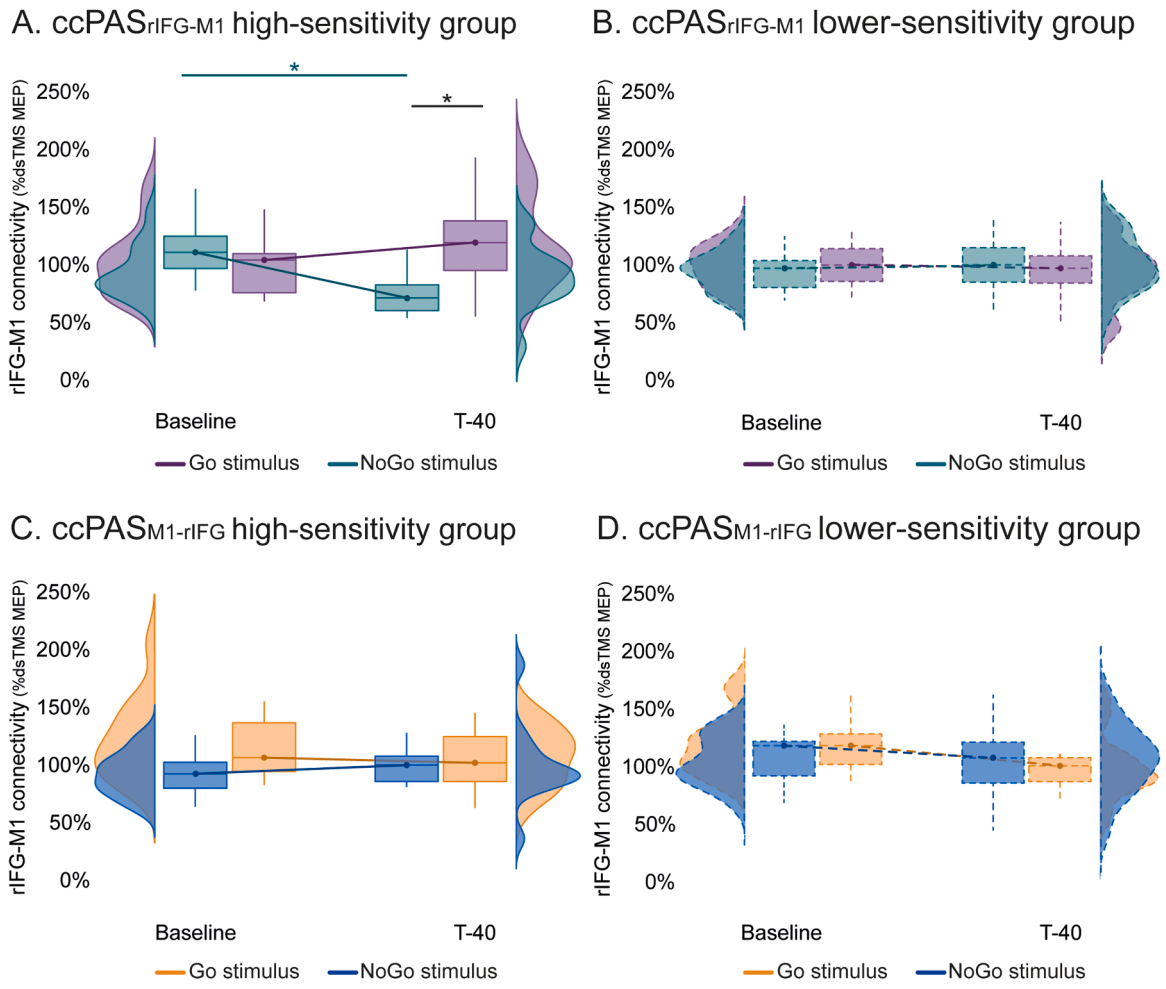

Fig. 4. Changes in %dsTMS-MEP amplitudes following $ccPAS_{rIFG-M1}$ in higher-sensitivity (**A**) and lower-sensitivity participants (**B**). Changes in %dsTMS-MEP amplitudes following $ccPAS_{M1\text{-}rIFG}$ in higher-sensitivity (**C**) and lower-sensitivity participants (**D**). Box plots represent the mean, first and third quartiles, and the 95 % confidence interval of individual data points. Half violins represent data distribution. Asterisks indicate significant post-hoc comparison: * = $p \leq .05$.

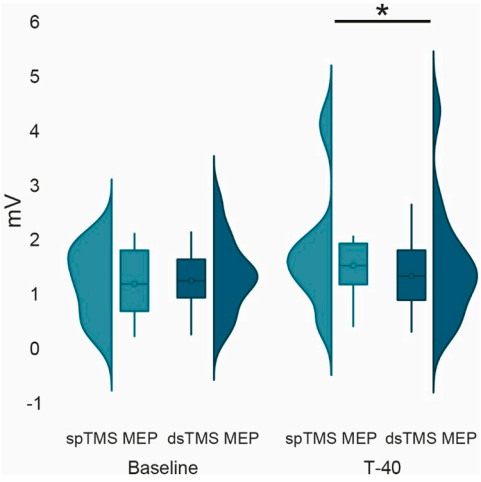

Fig. 5. spTMS- and dsTMS-MEP amplitudes (in mV) recorded during the vision of NoGo visual cues in high-sensitivity participants before (Baseline) and following (T40) $ccPAS_{rIFG-M1}$. Box plots represent the mean, first and third quartiles, and the 95 % confidence interval of individual data points. Half-violins represent data distribution. Asterisks indicate significant post-hoc comparison: * = $p \leq .05$.

monkeys (Mirabella et al., 2011) and human electrocorticographic studies (Mattia et al., 2012) have demonstrated that motor cortical activity is suppressed during motor inhibitory tasks. Prior dsTMS studies suggest that this suppression reflects the inhibitory effect of rIFG on M1 during action control, stopping, and reprogramming (Buch et al., 2010; Neubert et al., 2010; van Campen et al., 2013; Picazio et al., 2014). Here, we investigate whether transiently enhancing Hebbian-like associative plasticity along the rIFG-to-M1 pathway with ccPAS would alter neural responses and behavior during a Go-NoGo task.

5.1. *Direction-specific changes in motor excitability during ccPAS*

The analysis of conditioned MEPs recorded during the administration of the ccPAS protocol revealed an effect of stimulation directionality over time (Arai et al., 2011; Turrini et al., 2022, 2024; Bevacqua et al., 2024). Following the Hebbian principle (Hebb, 1949; Caporale and Dan, 2008), during the $ccPAS_{rIFG-M1}$, in which the input cortical site (rIFG) was repeatedly stimulated before the output cortical site (M1), we observed a progressive increase in the conditioned MEP amplitudes. This is consistent with previous work reporting progressive facilitation during ccPAS over premotor-M1 pathways (Arai et al., 2011; Turrini et al., 2022, 2023a, 2023b, 2024; Bevacqua et al., 2024), which can also persist after the end of the protocol (Lazari et al., 2022; Turrini et al., 2023). In contrast, we did not observe any significant differences in conditioned MEPs during ccPAS when we reversed the stimulation order ($ccPAS_{M1\text{-}rIFG}$). This result indicates that only $ccPAS_{rIFG-M1}$ was effective in inducing Hebbian STDP-like plasticity, consistent with a long-term

potentiation-like effect (Bi and Poo, 2001). However, the magnitude of this effect was highly variable across participants. Considering the growing evidence of interindividual variability in responses to non-invasive brain stimulation techniques (Hamada et al., 2013; López-Alonso et al., 2014), we chose to take into account the effectiveness of the ccPAS protocol, classifying our participants into higher- and lower-sensitivity groups based on the magnitude of the physiological modulation of the conditioned MEPs during $ccPAS_{rIFG\text{-}M1}$. We therefore selected the increase in MEP amplitude during $ccPAS_{rIFG\text{-}M1}$ as an index of sensitivity, as prior ccPAS and PAS literature has identified this index as a proxy for the effectiveness of the protocol (Turrini et al., 2023a,b; Guidali and Bolognini, 2025).

5.2. Direction-specific, state-dependent modulation of effective connectivity in higher-sensitivity individuals

Our main neurophysiological finding is a state-dependent modulation of effective connectivity following $ccPAS_{rIFG\text{-}M1}$, expressed only in higher-sensitivity participants: at T-40, dsTMS-MEPs were reduced when viewing NoGo cues relative to baseline, with no reliable change for Go cues. Importantly, spTMS-MEPs did not differ across timepoints, suggesting that the observed effect reflects changes in cortico-cortical influence (rIFG conditioning over left M1) rather than nonspecific shifts in corticospinal excitability. A direct comparison of spTMS and dsTMS MEPs at T-40 during NoGo cue presentation indicated lower dsTMS-MEP amplitudes than spTMS-MEPs in the higher-sensitivity group, consistent with strengthened inhibitory impact from IFG to M1 when contextual cues signal that an action should be withheld, even in the absence of any overt motor task. This pattern suggests that $ccPAS_{rIFG\text{-}M1}$ did not induce a global increase in excitability, but rather biased the functional influence of rIFG over M1 in a state-dependent manner.

In this framework, the progressive increase in conditioned MEPs observed during $ccPAS_{rIFG\text{-}M1}$ and the subsequent reduction in dsTMS-MEPs during NoGo cue processing can be interpreted as reflecting two complementary aspects of the same plasticity process. During $ccPAS_{rIFG\text{-}M1}$, stimulation was delivered at rest, and the gradual increase in conditioned MEP amplitudes provides an online index of the build-up of Hebbian STDP-like plasticity within the targeted pathway (Turrini et al., 2022). Importantly, only the subgroup of participants showing this online physiological evidence of pathway plasticity (i.e., higher-sensitivity participants) subsequently exhibited a state-dependent change in effective connectivity following $ccPAS_{rIFG\text{-}M1}$. In this context, changes in dsTMS-MEPs reflect the context-dependent expression of this plasticity, such that rIFG exerts a stronger inhibitory influence over M1 when processing visual cues associated with action withholding. Thus, ccPAS-induced plasticity does not translate into a uniform change in cortical excitability, but rather into a context-dependent reweighting of rIFG-M1 interactions. This interpretation aligns with previous dsTMS studies showing that the influence of premotor and prefrontal regions on M1 dynamically shifts depending on behavioral context (Davare et al., 2009; Buch et al., 2010; Neubert et al., 2010; Picazio et al., 2014).

No comparable modulation emerged after $ccPAS_{M1\text{-}rIFG}$ or in lower-sensitivity participants, suggesting that the observed physiological changes were selective both in terms of pathway directionality and participant subgroup. The fact that the effect was present only after $ccPAS_{rIFG\text{-}M1}$, and not after the reversed $ccPAS_{M1\text{-}rIFG}$ protocol, is consistent with the idea that the rIFG-to-M1 pathway is the relevant route for this inhibitory modulation under the present behavioral context and stimulation parameters. Likewise, its restriction to higher-sensitivity participants indicates that only individuals showing measurable plasticity during the ccPAS session subsequently expressed this NoGo-specific change in effective connectivity. The absence of modulation in lower-sensitivity participants implies that, in these individuals, the stimulation did not produce sufficient strengthening of the pathway to alter its state-dependent influence, at least within the temporal window and task context tested here.

Our findings suggest that rIFG projections to left M1 are more involved in action inhibition than in attentional allocation, as the rIFG-to-M1 pathway showed an inhibitory dsTMS MEP modulation only when processing NoGo stimuli associated with the suppression of prepotent motor responses. This suggests that the influence of rIFG over left M1 was dynamically adjusted in a state-dependent manner, enhancing inhibition specifically when seeing stimuli associated with action withholding. In contrast, our data do not reveal any significant difference in dsTMS-MEPs during the observation of the Go stimulus, implying that, in our experimental framework, the rIFG-to-M1 pathway does not appear to have a generalized role in motor control. Instead, its function may be more specifically related to action suppression rather than overall motor regulation. These results reinforce the model of rIFG as a top-down controller of motor output, rather than a mere salience or attentional hub, and provide a framework for future interventions aimed at improving inhibitory control.

From a mechanistic perspective, the physiological effect we observed – a NoGo-specific reduction in dsTMS-MEPs observed only in higher-sensitivity individuals – may indicate that in some participants, the rIFG-to-M1 pathway can be biased toward greater inhibitory control when environmental cues signal the need to withhold action. This aligns with models of context-dependent inhibitory gating in which prefrontal-motor projections adjust their influence in anticipation of specific action requirements (Duque et al., 2017; Wessel and Aron, 2017). It should be noted that, in our design, this modulation was measured during passive cue observation in the dsTMS blocks, rather than during active NoGo performance. Thus, it may reflect stimulus-triggered inhibitory priming rather than the execution of an overt inhibitory command.

A further point to consider is that these neurophysiological changes were assessed at T40, after three intervening Go-NoGo task blocks performed since baseline. Hence, any physiological effect measured at this stage must be interpreted in light of repeated task execution. Nevertheless, the observed pattern is unlikely to reflect a simple practice-related effect, as such effects typically consist of an increase in corticospinal excitability (e.g., Bütefisch et al., 2000; Lee et al., 2010), whereas in our study spTMS-MEPs remained unchanged. Moreover, the observed MEP modulations were present only after $ccPAS_{rIFG\text{-}M1}$ and only in higher-sensitivity participants, with no comparable effects after $ccPAS_{M1\text{-}rIFG}$ or in lower-sensitivity participants, despite identical task exposure across sessions and groups. More generally, unlike classical use-dependent paradigms based on continuous repetition of the same motor output, response execution in our task occurred under sustained competition with response inhibition, making a pure use-dependent facilitation account unlikely.

5.3. Behavioral findings and trait-like differences in proactive inhibitory control

Remarkably, we found no evidence that ccPAS directly influenced behavioral performance in the Go-NoGo task. Across sessions, participants showed faster RTs and improved Go-trial accuracy (fewer omission errors), indicating enhanced response readiness. However, this was accompanied by more commission errors on NoGo trials, reflecting a shift toward a more impulsive response style in which responses became faster at the expense of inhibitory control, consistent with a speed-accuracy trade-off (Forstmann et al., 2008; Bogacz et al., 2010). In the context of Go-NoGo paradigms, such a pattern typically reflects reduced efficiency in proactive motor inhibition (Aron, 2011; Wessel and Aron, 2017), where participants become less able to implement a preparatory strategy that facilitates response suppression when a NoGo cue is presented. This trade-off became particularly informative when participants were stratified by ccPAS sensitivity: higher-sensitivity participants maintained a more effective proactive strategy, preserving commission error rates despite becoming faster. In contrast, lower-sensitivity participants failed to adopt an adaptive proactive strategy, showing increased response speed accompanied by a deterioration in reactive

inhibition accuracy, as reflected by the increase in commission errors.

Critically, however, ccPAS did not produce a direct group-level change in any behavioral measure. The behavioral difference between higher- and lower-sensitivity participants emerged after both $ccPAS_{M1\text{-}rIFG}$ and $ccPAS_{rIFG\text{-}M1}$, making it unlikely to result from the ccPAS-targeted intervention. Instead, it more plausibly reflects a trait-like predisposition, whereby individuals capable of expressing greater ccPAS-induced Hebbian-like plasticity in the rIFG-to-M1 pathway also tend to maintain a more favorable speed-accuracy balance during practice. The preservation of proactive inhibitory control in the higher-sensitivity group nonetheless parallels our physiological finding of NoGo-specific modulation of IFG-to-M1 connectivity in the same subgroup following $ccPAS_{rIFG\text{-}M1}$, suggesting that both effects may reflect a common underlying property of this pathway rather than a direct consequence of stimulation.

Thus, while our findings do not demonstrate a causal effect of ccPAS on behavior, they highlight an association between individual plasticity capacity and behavioral profile. Importantly, the present data do not allow us to determine whether such variability reflects a general propensity for plasticity across different stimulation protocols or a more specific property of the rIFG-M1 pathway targeted here. The pattern of results is more directly consistent with the latter interpretation, as both the physiological and behavioral differences selectively involved this circuit. Accordingly, we interpret ccPAS sensitivity as a putative marker of the capacity of the rIFG-M1 pathway to express Hebbian-like plasticity, which may be functionally related to individual differences in proactive inhibitory control. More in general, our results are consistent with prior evidence that interindividual variability in responsiveness to neuromodulation can track stable differences in cognitive-motor performance (Turrini et al., 2023a), and with proposals that network plasticity may reflect more efficient functional engagement of the underlying circuitry (Freitas et al., 2013; Stampanoni Bassi et al., 2019; Di Luzio et al., 2024). Individuals with greater plastic potential in the rIFG-to-M1 pathway may be better able to maintain effective proactive inhibitory control over time while improving response efficiency. This is also consistent with prior work suggesting that individual variability in ccPAS-induced plasticity predicts behavioral outcomes such as changes in motor accuracy or learning (Turrini et al., 2023a, 2023b; Bevacqua et al., 2024).

Variability in responsiveness to TMS interventions is influenced by several factors, such as individual characteristics, stimulation parameters, and ongoing brain activity (Cheeran et al., 2008; Antal et al., 2010; Conde et al., 2012; Lee et al., 2018; Corp et al., 2021). We can speculate that in our experiment, the application of a fixed interstimulus interval during ccPAS or standardized stimulation coordinates across all participants may have limited the efficacy of the ccPAS protocol in some individuals (Karabanov et al., 2013; Corp et al., 2021). Emerging evidence suggests that more tailored approaches could improve response consistency and specificity (Chiappini et al., 2018; Goldenkoff et al., 2024; Turrini et al., 2025). Future work using tailored ccPAS approaches, for example, aligning stimulation with task-relevant oscillatory activity implicated in motor inhibition (Schmidt et al., 2019; Wessel and Anderson, 2024) may improve the reliability and specificity of IFG-to-M1 neuromodulatory interventions (Zrenner and Ziemann, 2024).

5.4. Limitations and concluding remarks

Our study has limitations. Firstly, we did not use a sham stimulation as a control condition, which precluded us from characterizing participants' behavior with no active ccPAS. Additionally, we focused exclusively on rIFG. Although the prevailing functional model of motor inhibition emphasizes right-hemisphere dominance (Aron, 2011), more recent evidence suggests that successful action inhibition also requires engagement of the left hemisphere (Swick et al., 2008; Mirabella et al., 2017; Di Caprio et al., 2020). Future research should further explore the functional role of the connections between the left IFG and left/right M1 in motor inhibition, to better understand the contribution of left-hemispheric circuits to inhibitory control mechanisms. A further limitation concerns the interpretation of interindividual differences in ccPAS responsiveness. The present design does not allow us to fully disentangle whether higher sensitivity reflects a general propensity for plasticity, a pathway-specific property of the rIFG–M1 circuit, or a sensitivity to the ccPAS protocol itself. This issue cannot be resolved in the absence of additional control conditions targeting different networks or involving different stimulation protocols.

The current results support the view that rIFG can exert inhibitory control over the left M1 via a cortico-cortical pathway. Selective modulation of the pathway connecting rIFG to M1 via Hebbian-like plasticity produced a NoGo-specific reduction in effective connectivity in higher-sensitivity participants, consistent with enhanced top-down inhibition in contexts associated with action withholding. Although ccPAS did not elicit a direct, group-level change in Go-NoGo performance, individual differences in physiological sensitivity to $ccPAS_{rIFG\text{-}M1}$ were associated with different behavioral profiles during task execution: individuals expressing greater plasticity during ccPAS maintained a good inhibitory accuracy while responding faster, showing a better proactive strategy. The marked heterogeneity in ccPAS responsiveness highlights the importance of identifying factors that shape individual sensitivity to neuromodulation. Accounting for such factors may improve the reliability and specificity of ccPAS-based interventions and inform future applications targeting disorders characterized by deficits in inhibitory control.

Funding

This work was supported by two Bial Foundation grants [304/2022 and 346/2024] awarded to AA. Additional support was provided by the PRIN 2022 project [2022NEE53Z], funded by the Italian Ministry of University and Research (MUR); the Universidad Católica Del Maule [CDPDS2022]; FISM—Fondazione Italiana Sclerosi Multipla [2022/R-Single/071], financed or cofinanced with the "5‰" public funding; and Fondazione del Monte di Bologna e Ravenna [1402bis/2021] all awarded to AA. GA and SZ were funded by the Ministry of Health [Ricerca Corrente 2023]. GM was supported by the Department of Clinical and Experimental Sciences of the University of Brescia under the Project "Departments of Excellence 2023–2027" (IN2DEPT – Innovative and Integrative Department Platforms) and by the PRIN 2022 project [20225PFP7L]. The authors gratefully acknowledge these supports.

Data availability

The data that support the findings of this study are openly available in OSF at https://osf.io/7wjd3/.

CRediT authorship contribution statement

Naomi Bevacqua: Writing – review & editing, Writing – original draft, Visualization, Methodology, Investigation, Formal analysis, Data curation. **Sonia Turrini:** Writing – review & editing, Writing – original draft, Software, Methodology, Investigation. **Antonio Cataneo:** Writing – review & editing, Investigation. **Sara Zago:** Writing – review & editing, Funding acquisition. **Giorgio Arcara:** Writing – review & editing, Funding acquisition. **Matteo Candidi:** Writing – review & editing, Supervision. **Giovanni Mirabella:** Writing – review & editing, Writing – original draft, Funding acquisition, Formal analysis. **Alessio Avenanti:** Writing – review & editing, Writing – original draft, Supervision, Project administration, Methodology, Funding acquisition, Conceptualization.

Declaration of competing interest

The authors do not have any conflicts of interest to disclose.

References

Antal, A., Chaieb, L., Moliadze, V., Monte-Silva, K., Poreisz, C., Thirugnanasambandam, N., Nitsche, M.A., Shoukier, M., Ludwig, H., Paulus, W., 2010. Brain-derived neurotrophic factor (*BDNF*) gene polymorphisms shape cortical plasticity in humans. Brain Stimul. 3, 230–237.

Arai, N., Müller-Dahlhaus, F., Murakami, T., Bliem, B., Lu, M.-K., Ugawa, Y., Ziemann, U., 2011. State-dependent and timing-dependent bidirectional associative plasticity in the human SMA-M1 network. J. Neurosci. 31, 15376–15383.

Arlati, N., Però, L., Lenzi, L., Quettier, T., Ippolito, G., Battaglia, S., Borgomaneri, S., 2026. Online corticomotor modulations in action inhibition: insights from TMS studies. J. Affect. Disord. 396, 120825.

Aron, A.R., 2011. From reactive to proactive and selective control: developing a richer model for stopping inappropriate responses. Biol. Psychiatry 69.

Aron, A.R., Robbins, T.W., Poldrack, R.A., 2014. Inhibition and the right inferior frontal cortex: one decade on. Trends Cogn. Sci. 18, 177–185.

Bari, A., Robbins, T.W., 2013. Inhibition and impulsivity: behavioral and neural basis of response control. Prog. Neurobiol. 108, 44–79.

Bäumer, T., Schippling, S., Kroeger, J., Zittel, S., Koch, G., Thomalla, G., Rothwell, J.C., Siebner, H.R., Orth, M., Münchau, A., 2009. Inhibitory and facilitatory connectivity from ventral premotor to primary motor cortex in healthy humans at rest – a bifocal TMS study. Clin. Neurophysiol. 120, 1724–1731.

Bevacqua, N., Turrini, S., Avenanti, A., 2026. Optimal parameters for reliable PMv–M1 facilitation identified with dual coil TMS. Clin. Neurophysiol. 181, 2111434.

Bevacqua, N., Turrini, S., Fiori, F., Saracini, C., Lucero, B., Candidi, M., Avenanti, A., 2024. Cortico-cortical paired associative stimulation highlights asymmetrical communication between rostral premotor cortices and primary motor cortex. Brain Stimul. 17, 89–91.

Bi, G., Poo, M., 2001. Synaptic modification by correlated activity: Hebb's Postulate revisited. Annu. Rev. Neurosci. 24, 139–166.

Bogacz, R., Wagenmakers, E.-J., Forstmann, B.U., Nieuwenhuis, S., 2010. The neural basis of the speed–accuracy tradeoff. Trends Neurosci. 33, 10–16.

Borgomaneri, S., Serio, G., Battaglia, S., 2020. Please, don't do it! fifteen years of progress of non-invasive brain stimulation in action inhibition. Cortex 132, 404–422.

Buch, E.R., Johnen, V.M., Nelissen, N., O'Shea, J., Rushworth, M.F.S., 2011. Noninvasive associative plasticity induction in a corticocortical pathway of the human brain. J. Neurosci. 31, 17669–17679.

Buch, E.R., Mars, R.B., Boorman, E.D., Rushworth, M.F.S., 2010. A network centered on ventral premotor cortex exerts both facilitatory and inhibitory control over primary motor cortex during action reprogramming. J. Neurosci. 30, 1395–1401.

Bütefisch, C.M., Davis, B.C., Wise, S.P., Sawaki, L., Kopylev, L., Classen, J., Cohen, L.G., 2000. Mechanisms of use-dependent plasticity in the human motor cortex. Proc. Natl. Acad. Sci. U.S.A. 97, 3661–3665.

Caporale, N., Dan, Y., 2008. Spike timing-dependent plasticity: a Hebbian learning rule. Annu. Rev. Neurosci. 31, 25–46.

Chao, C.C., Karabanov, A.N., Paine, R., de Campos, A.C., Kukke, S.N., Wu, T., Wang, H., Hallett, M., 2015. Induction of motor associative plasticity in the posterior parietal cortex-primary motor network. Cereb. Cortex 25, 365–373.

Cheeran, B., Talelli, P., Mori, F., Koch, G., Suppa, A., Edwards, M., Houlden, H., Bhatia, K., Greenwood, R., Rothwell, J.C., 2008. A common polymorphism in the brain-derived neurotrophic factor gene (BDNF) modulates human cortical plasticity and the response to rTMS. J. Physiol. 586, 5717–5725.

Chiappini, E., Borgomaneri, S., Marangon, M., Turrini, S., Romei, V., Avenanti, A., 2020. Driving associative plasticity in premotor-motor connections through a novel paired associative stimulation based on long-latency cortico-cortical interactions. Brain Stimul. 13, 1461–1463.

Chiappini, E., Silvanto, J., Hibbard, P.B., Avenanti, A., Romei, V., 2018. Strengthening functionally specific neural pathways with transcranial brain stimulation. Curr. Biol. 28, R735–R736.

Chiappini, E., Turrini, S., Fiori, F., Benassi, M., Tessari, A., di Pellegrino, G., Avenanti, A., 2025. You are as old as the connectivity You keep: distinct neurophysiological mechanisms underlying age-related changes in hand dexterity and strength. Arch. Med. Res. 56, 103031.

Chiappini, E., Turrini, S., Zanon, M., Marangon, M., Borgomaneri, S., Avenanti, A., 2024. Driving hebbian plasticity over ventral premotor-motor projections transiently enhances motor resonance. Brain Stimul. 17, 211–220.

Conde, V., Vollmann, H., Sehm, B., Taubert, M., Villringer, A., Ragert, P., 2012. Cortical thickness in primary sensorimotor cortex influences the effectiveness of paired associative stimulation. Neuroimage 60, 864–870.

Corp, D.T., Bereznicki, H.G.K., Clark, G.M., Youssef, G.J., Fried, P.J., Jannati, A., Davies, C.B., Gomes-Osman, J., Kirkovski, M., Albein-Urios, N., Fitzgerald, P.B., Koch, G., Di Lazzaro, V., Pascual-Leone, A., Enticott, P.G., 2021. Large-scale analysis of interindividual variability in single and paired-pulse TMS data. Clin. Neurophysiol. 132, 2639–2653.

Davare, M., Lemon, R., Olivier, E., 2008. Selective modulation of interactions between ventral premotor cortex and primary motor cortex during precision grasping in humans. J. Physiol. 586, 2735–2742.

Davare, M., Montague, K., Olivier, E., Rothwell, J.C., Lemon, R.N., 2009. Ventral premotor to primary motor cortical interactions during object-driven grasp in humans. Cortex 45, 1050–1057.

Davare, M., Rothwell, J.C., Lemon, R.N., 2010. Causal connectivity between the Human anterior intraparietal area and premotor cortex during grasp. Curr. Biol. 20, 176–181.

Devanne, H., Lavoie, B.A., Capaday, C., 1997. Input-output properties and gain changes in the human corticospinal pathway. Exp. Brain Res. 114, 329–338.

Di Caprio, V., Modugno, N., Mancini, C., Olivola, E., Mirabella, G., 2020. Early-stage Parkinson's patients show selective impairment in reactive but not proactive inhibition. Movement Disord. 35, 409–418.

Di Lazzaro, V., Oliviero, A., Pilato, F., Saturno, E., Dileone, M., Mazzone, P., Insola, A., Tonali, P.A., Rothwell, J.C., 2004. The physiological basis of transcranial motor cortex stimulation in conscious humans. Clin. Neurophysiol. 115, 255–266.

Di Luzio, P., Brady, L., Turrini, S., Romei, V., Avenanti, A., Sel, A., 2024. Investigating the effects of cortico-cortical paired associative stimulation in the human brain: a systematic review and meta-analysis. Neurosci. Biobehav. Rev. 167, 105933.

Duque, J., Greenhouse, I., Labruna, L., Ivry, R.B., 2017. Physiological markers of motor inhibition during Human behavior. Trends Neurosci. 40, 219–236.

Fiebelkorn, I.C., Kastner, S., 2019. A rhythmic theory of attention. Trends Cogn. Sci. 23, 87–101.

Fiori, F., Chiappini, E., Avenanti, A., 2018. Enhanced action performance following TMS manipulation of associative plasticity in ventral premotor-motor pathway. Neuroimage 183, 847–858.

Fiori, F., Chiappini, E., Candidi, M., Romei, V., Borgomaneri, S., Avenanti, A., 2017. Long-latency interhemispheric interactions between motor-related areas and the primary motor cortex: a dual site TMS study. Sci. Rep. 7, 14936.

Fiori, F., Chiappini, E., Soriano, M., Paracampo, R., Romei, V., Borgomaneri, S., Avenanti, A., 2016. Long-latency modulation of motor cortex excitability by ipsilateral posterior inferior frontal gyrus and pre-supplementary motor area. Sci. Rep. 6, 38396.

Forstmann, B.U., Dutilh, G., Brown, S., Neumann, J., von Cramon, D.Y., Ridderinkhof, K. R., Wagenmakers, E.-J., 2008. Striatum and pre-SMA facilitate decision-making under time pressure. Proc. Natl. Acad. Sci. U.S.A. 105, 17538–17542.

Freitas, C., Farzan, F., Pascual-Leone, A., 2013. Assessing brain plasticity across the lifespan with transcranial magnetic stimulation: why, how, and what is the ultimate goal? Front. Neurosci. 7, 42.

Goldenkoff, E.R., Deluisi, J.A., Lee, T.G., Hampstead, B.M., Taylor, S.F., Polk, T.A., Vesia, M., 2024. Repeated spaced cortical paired associative stimulation promotes additive plasticity in the human parietal-motor circuit. Clin. Neurophysiol. 166, 202–210.

Guidali, G., Bolognini, N., 2025. Tracking changes in corticospinal excitability during visuomotor paired associative stimulation to predict motor resonance rewriting. Brain Sci. 15, 257.

Hamada, M., Murase, N., Hasan, A., Balaratnam, M., Rothwell, J.C., 2013. The role of interneuron networks in driving Human motor cortical plasticity. Cereb. Cortex. 23, 1593–1605.

Hampshire, A., Chamberlain, S.R., Monti, M.M., Duncan, J., Owen, A.M., 2010. The role of the right inferior frontal gyrus: inhibition and attentional control. Neuroimage 50, 1313–1319.

Hamzei, F., Dettmers, C., Rzanny, R., Liepert, J., Büchel, C., Weiller, C., 2002. Reduction of excitability ("Inhibition") in the ipsilateral primary motor cortex is mirrored by fMRI signal decreases. Neuroimage 17, 490–496.

He, Q., Geißler, C.F., Ferrante, M., Hartwigsen, G., Friehs, M.A., 2024. Effects of transcranial magnetic stimulation on reactive response inhibition. Neurosci. Biobehav. Rev. 157, 105532.

Hebb, D.O., 1949. The Organization of Behavior; A Neuropsychological Theory. Wiley, Oxford, England.

Hernandez-Pavon, J.C., San Agustín, A., Wang, M.C., Veniero, D., Pons, J.L., 2023. Can we manipulate brain connectivity? A systematic review of cortico-cortical paired associative stimulation effects. Clin. Neurophysiol. 154, 169–193.

Johnen, V.M., Neubert, F.X., Buch, E.R., Verhagen, L.M., O'Reilly, J., Mars, R.B., Rushworth, M.F.S., 2015. Causal manipulation of functional connectivity in a specific neural pathway during behaviour and at rest. Elife 4, e04585.

Kammer, T., Beck, S., Thielscher, A., Laubis-Herrmann, U., Topka, H., 2001. Motor thresholds in humans: a transcranial magnetic stimulation study comparing different pulse waveforms, current directions and stimulator types. Clin. Neurophysiol. 112, 250–258.

Karabanov, A.N., Chao, C.C., Paine, R., Hallett, M., 2013. Mapping different intra-hemispheric parietal-motor networks using twin coil TMS. Brain Stimul. 6, 384–389.

Koch, G., 2020. Cortico-cortical connectivity: the road from basic neurophysiological interactions to therapeutic applications. Exp. Brain Res. 238, 1677–1684.

Lazari, A., Salvan, P., Cottaar, M., Papp, D., Rushworth, M.F.S., Johansen-Berg, H., 2022. Hebbian activity-dependent plasticity in white matter. Cell Rep. 39, 110951.

Lee, M., Hinder, M.R., Gandevia, S.C., Carroll, T.J., 2010. The ipsilateral motor cortex contributes to cross-limb transfer of performance gains after ballistic motor practice. J. Physiol. 588, 201–212.

Lee, E.G., Rastogi, P., Hadimani, R.L., Jiles, D.C., Camprodon, J.A., 2018. Impact of non-brain anatomy and coil orientation on inter- and intra-subject variability in TMS at midline. Clin. Neurophysiol. 129, 1873–1883.

López-Alonso, V., Cheeran, B., Río-Rodríguez, D., Fernández-del-Olmo, M., 2014. Inter-individual variability in response to non-invasive brain stimulation paradigms. Brain Stimul. 7, 372–380.

Lu, M.-K., Tsai, C.-H., Ziemann, U., 2012. Cerebellum to motor cortex paired associative stimulation induces bidirectional STDP-like plasticity in human motor cortex. Front. Hum. Neurosci. 6, 260.

Mattia, M., Spadacenta, S., Pavone, L., Quarato, P., Esposito, V., Sparano, A., Sebastiano, F., Di Gennaro, G., Morace, R., Cantore, G., Mirabella, G., 2012. Stop-event-related potentials from intracranial electrodes reveal a key role of premotor and motor cortices in stopping ongoing movements. Front. Neuroeng. 5, 12.

Mayka, M.A., Corcos, D.M., Leurgans, S.E., Vaillancourt, D.E., 2006. Three-dimensional locations and boundaries of motor and premotor cortices as defined by functional brain imaging: a meta-analysis. Neuroimage 31, 1453–1474.

Mirabella, G., 2023. Beyond reactive inhibition: unpacking the multifaceted nature of motor inhibition. Brain Sci. 13, 804.
Mirabella, G., Fragola, M., Giannini, G., Modugno, N., Lakens, D., 2017. Inhibitory control is not lateralized in Parkinson's patients. Neuropsychologia 102, 177–189.
Mirabella, G., Pani, P., Ferraina, S., 2011. Neural correlates of cognitive control of reaching movements in the dorsal premotor cortex of rhesus monkeys. J. Neurophysiol. 106, 1454–1466.
Neubert, F.X., Mars, R.B., Buch, E.R., Olivier, E., Rushworth, M.F.S., 2010. Cortical and subcortical interactions during action reprogramming and their related white matter pathways. Proc. Natl. Acad. Sci. U.S.A. 107, 13240–13245.
Oldfield, R.C., 1971. The assessment and analysis of handedness: the Edinburgh inventory. Neuropsychologia 9, 97–113.
Paracampo, R., Pirruccio, M., Costa, M., Borgomaneri, S., Avenanti, A., 2018. Visual, sensorimotor and cognitive routes to understanding others' enjoyment: an individual differences rTMS approach to empathic accuracy. Neuropsychologia 116, 86–98.
Picazio, S., Veniero, D., Ponzo, V., Caltagirone, C., Gross, J., Thut, G., Koch, G., 2014. Prefrontal control over motor cortex cycles at beta frequency during movement inhibition. Curr. Biol. 24, 2940–2945.
Prochnow, A., Wendiggensen, P., Eggert, E., Münchau, A., Beste, C., 2022. Pre-trial fronto-occipital electrophysiological connectivity affects perception–action integration in response inhibition. Cortex 152, 122–135.
Ren, Q., Gentsch, A., Kaiser, J., Schütz-Bosbach, S., 2023. Ready to go: higher sense of agency enhances action readiness and reduces response inhibition. Cognition 237, 105456.
Ridderinkhof, K.R., van den Wildenberg, W.P.M., Segalowitz, S.J., Carter, C.S., 2004. Neurocognitive mechanisms of cognitive control: the role of prefrontal cortex in action selection, response inhibition, performance monitoring, and reward-based learning. Brain Cogn. 56, 129–140.
Rizzo, V., Siebner, H.S., Morgante, F., Mastroeni, C., Girlanda, P., Quartarone, A., 2009. Paired associative stimulation of left and right human motor cortex shapes interhemispheric motor inhibition based on a Hebbian mechanism. Cereb. Cortex 19, 907–915.
Rossi, S., Santarnecchi, E., Feurra, M., 2022. Noninvasive brain stimulation and brain oscillations. Handb. Clin. Neurol. 184, 239–247.
Rossini, P.M., et al., 2015. Non-invasive electrical and magnetic stimulation of the brain, spinal cord, roots and peripheral nerves: basic principles and procedures for routine clinical and research application: an updated report from an I.F.C.N. Committee. Clin. Neurophysiol. 126, 1071–1107.
Schmidt, R., Ruiz, M.H., Kilavik, B.E., Lundqvist, M., Starr, P.A., Aron, A.R., 2019. Beta oscillations in working memory, executive control of movement and thought, and sensorimotor function. J. Neurosci. 39, 8231–8238.
Sebastian, A., Jung, P., Neuhoff, J., Wibral, M., Fox, P.T., Lieb, K., Fries, P., Eickhoff, S.B., Tüscher, O., Mobascher, A., 2016. Dissociable attentional and inhibitory networks of dorsal and ventral areas of the right inferior frontal cortex: a combined task-specific and coordinate-based meta-analytic fMRI study. Brain Struct. Funct. 221, 1635–1651.
Sel, A., Verhagen, L., Angerer, K., David, R., Klein-Flügge, M.C., Rushworth, M.F.S., 2021. Increasing and decreasing interregional brain coupling increases and decreases oscillatory activity in the human brain. Proc. Natl. Acad. Sci. U.S.A. 118, e2100652118.
Stampanoni Bassi, M., Iezzi, E., Gilio, L., Centonze, D., Buttari, F., 2019. Synaptic plasticity shapes brain connectivity: implications for network topology. Int. J. Mol. Sci. 20, 6193.
Stinear, C.M., Coxon, J.P., Byblow, W.D., 2009. Primary motor cortex and movement prevention: where stop meets go. Neurosci. Biobehav. Rev. 33, 662–673.
Swann, N.C., Cai, W., Conner, C.R., Pieters, T.A., Claffey, M.P., George, J.S., Aron, A.R., Tandon, N., 2012. Roles for the pre-supplementary motor area and the right inferior frontal gyrus in stopping action: electrophysiological responses and functional and structural connectivity. Neuroimage 59, 2860–2870.
Swick, D., Ashley, V., Turken, A.U., 2008. Left inferior frontal gyrus is critical for response inhibition. BMC. Neurosci. 9, 102.
Tomaiuolo, F., MacDonald, J.D., Caramanos, Z., Posner, G., Chiavaras, M., Evans, A.C., Petrides, M., 1999. Morphology, morphometry and probability mapping of the pars opercularis of the inferior frontal gyrus: an in vivo MRI analysis. Eur. J. Neurosci. 11, 3033–3046.
Tomczak, M., Tomczak, E., 2014. The need to report effect size estimates revisited. An overview of some recommended measures of effect size. Trends Sport Sci. 1, 19–25.
Trajkovic, J., Romei, V., Rushworth, M.F.S., Sel, A., 2023. Changing connectivity between premotor and motor cortex changes inter-areal communication in the human brain. Prog. Neurobiol. 228, 102487.
Turrini, S., 2023. MEPautomatedanalysis (Version 1.1). Available at: https://github.com/SoniaTurrini/MEPautomatedanalysis.git.
Turrini, S., Bevacqua, N., Cataneo, A., Chiappini, E., Fiori, F., Battaglia, S., Romei, V., Avenanti, A., 2023a. Neurophysiological markers of premotor–motor network plasticity predict motor performance in young and older adults. Biomedicines 11, 1464.
Turrini, S., Bevacqua, N., Cataneo, A., Chiappini, E., Fiori, F., Candidi, M., Avenanti, A., 2023b. Transcranial cortico-cortical paired associative stimulation (ccPAS) over ventral premotor-motor pathways enhances action performance and corticomotor excitability in young adults more than in elderly adults. Front. Aging Neurosci. 15, 1119508. Available at: https://www.frontiersin.org/articles/10.3389/fnagi.2023.1119508 [Accessed February 17, 2023].
Turrini, S., Fiori, F., Arcara, G., Romei, V., di Pellegrino, G., Avenanti, A., 2025. State-dependent associative plasticity highlights function-specific premotor-motor pathways crucial for arbitrary visuomotor mapping. Sci. Adv. 11, eadu4098.
Turrini, S., Fiori, F., Bevacqua, N., Saracini, C., Lucero, B., Candidi, M., Avenanti, A., 2024. Spike-timing-dependent plasticity induction reveals dissociable supplementary– and premotor–motor pathways to automatic imitation. Proc. Natl. Acad. Sci. U.S.A. 121, e2404925121.
Turrini, S., Fiori, F., Chiappini, E., Lucero, B., Santarnecchi, E., Avenanti, A., 2023c. Cortico-cortical paired associative stimulation (ccPAS) over premotor-motor areas affects local circuitries in the human motor cortex via Hebbian plasticity. Neuroimage 271, 120027.
Turrini, S., Fiori, F., Chiappini, E., Romei, V., Santarnecchi, E., Avenanti, A., 2022. Gradual enhancement of corticomotor excitability during cortico-cortical paired associative stimulation. Sci. Rep, 12, 14670.
Valchev, N., Tidoni, E., Hamilton AF de, C., Gazzola, V., Avenanti, A., 2017. Primary somatosensory cortex necessary for the perception of weight from other people's action: a continuous theta-burst TMS experiment. Neuroimage 152, 195–206.
Vallence, A.-M., Goldsworthy, M.R., Hodyl, N.A., Semmler, J.G., Pitcher, J.B., Ridding, M.C., 2015. Inter- and intra-subject variability of motor cortex plasticity following continuous theta-burst stimulation. Neuroscience 304, 266–278.
van Campen, A.D., Neubert, F.X., van den Wildenberg, W.P.M., Richard Ridderinkhof, K., Mars, R.B., 2013. Paired-pulse transcranial magnetic stimulation reveals probability-dependent changes in functional connectivity between right inferior frontal cortex and primary motor cortex during go/no-go performance. Front. Hum. Neurosci. 7, 736.
van den Wildenberg, W.P.M., Ridderinkhof, K.R., Wylie, S.A., 2022. Towards conceptual clarification of proactive inhibitory control: a review. Brain Sci. 12, 1638.
Van Malderen, S.V., Hehl, M., Verstraelen, S., Swinnen, S.P., Cuypers, K., 2023. Dual-site TMS as a tool to probe effective interactions within the motor network: a review. Rev. Neurosci. 34, 129–221.
Wessel, J.R., 2018. An adaptive orienting theory of error processing. Psychophysiology 55, e13041.
Wessel, J.R., Anderson, MC, 2024. Neural mechanisms of domain-general inhibitory control. Trends Cogn. Sci. 28, 124–143.
Wessel, J.R., Aron, A.R., 2017. On the globality of motor suppression: unexpected events and their influence on behavior and cognition. Neuron 93, 259–280.
WMA, 2013. World Medical Association Declaration of Helsinki: ethical principles for medical research involving human subjects. JAMA 310 (20), 2191–2194.
Young, M.E., Sutherland, S.C., McCoy, A.W., 2018. Optimal go/no-go ratios to maximize false alarms. Behav. Res. 50, 1020–1029.
Zrenner, C., Ziemann, U., 2024. Closed-loop brain stimulation. Biol. Psychiatry 95, 545–552.